Accepted Manuscript

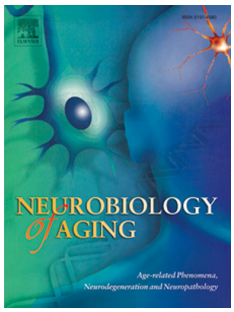

The miRNome of Alzheimer's disease: consistent downregulation of the miR-132/212 cluster

Sabrina Pichler, M.Sc., Wei Gu, Ph.D, Daniela Hartl, Ph.D, Gilles Gasparoni, Ph.D, Petra Leidinger, Ph.D, Andreas Keller, Prof, Chair of Clinical Bioinformatics, Eckart Meese, Prof, Manuel Mayhaus, Ph.D, Harald Hampel, M.D, Ph.D, MSc., Prof, Matthias Riemenschneider, M.D., Ph.D., Prof

PII: S0197-4580(16)30233-0

DOI: 10.1016/j.neurobiolaging.2016.09.019

Reference: NBA 9732

To appear in: *Neurobiology of Aging*

Received Date: 31 January 2016

Revised Date: 7 September 2016

Accepted Date: 24 September 2016

Please cite this article as: Pichler, S., Gu, W., Hartl, D., Gasparoni, G., Leidinger, P., Keller, A., Meese, E., Mayhaus, M., Hampel, H., Riemenschneider, M., The miRNome of Alzheimer's disease: consistent downregulation of the miR-132/212 cluster, *Neurobiology of Aging* (2016), doi: 10.1016/j.neurobiolaging.2016.09.019.

The miRNome of Alzheimer's disease: consistent downregulation of the miR-132/212 cluster

Sabrina Pichler (M.Sc.)[a], Wei Gu (Ph.D)[a,d], Daniela Hartl (Ph.D)[a], Gilles Gasparoni (Ph.D)[a], Petra Leidinger (Ph.D)[b], Andreas Keller (Prof)[c], Eckart Meese (Prof)[b], Manuel Mayhaus (Ph.D)[a], Harald Hampel (M.D, Ph.D, MSc., Prof)[f, g] and Matthias Riemenschneider (M.D., Ph.D., Prof)[a,e]

[a] Neurobiological Laboratory, Department of Psychiatry and Psychotherapy, Saarland University, Kirrberger Str. 1, 66421 Homburg, Germany
[b] Department of Human Genetics, Saarland University, Kirrberger Str. 1, 66421 Homburg, Germany
[c] Chair of Clinical Bioinformatics, Saarland University, Campus 66123 Saarbrücken, Germany
[d] Luxembourg Centre For Systems Biomedicine (LCSB), University of Luxembourg, Campus Belval, House of Biomedicine, 7, avenue des Hauts-Fourneaux, 4362 Esch-sur-Alzette, Luxembourg
[e] Department of Psychiatry and Psychotherapy, Saarland University Hospital, Kirrberger Str. 1, 66421 Homburg, Germany
[f] AXA Research Fund & UPMC Chair
[g] Sorbonne Universités, Université Pierre et Marie Curie, Paris 06, Institut de la Mémoire et de la Maladie d'Alzheimer (IM2A) & Institut du Cerveau et de la Moelle épinière (ICM), Département de Neurologie, Hôpital de la Pitié-Salpétrière, Paris, France

running title: *Downregulation of miR-132/212 in Alzheimer's disease*

keywords: *Alzheimer's disease; human cortical brain tissue; microRNA; mRNA; hsa-miR-132; hsa-miR-212*

Corresponding author

Sabrina Pichler
Neurobiological Laboratory
Department of Psychiatry and Psychotherapy
Saarland University
Kirrberger Str. 1

66421 Homburg, Germany

Phone: +49 (0)6841 1624111
Fax: +49 (0)6841 1624270

E-Mail: sabrina.pichler@uks.eu

ABSTRACT

MicroRNAs (miRNAs) are small non-coding RNA molecules, with essential functions in RNA silencing and post-transcriptional regulation of gene expression. MiRNAs appear to regulate the development and function of the nervous system. Alterations of miRNA expression have been associated with Alzheimer's disease (AD). To characterize the AD miRNA signature we examined genome wide miRNA and mRNA expression patterns in the temporal cortex of AD and control samples. We validated our miRNA results by semi-quantitative real-time PCR in independent prefrontal cortex. Further, we separated grey and white matter brain sections to identify the cellular origin of the altered miRNA expression. We observed genome wide downregulation of hsa-miR-132-3p and hsa-miR-212-3p in AD with a stronger decrease in grey matter AD samples. We further identified ten differently expressed transcripts achieving genome wide levels of significance. Significantly deregulated miRNAs and mRNAs were correlated and examined for potential binding sites *(in silico)*. This miRNome-wide study in AD provides supportive evidence and corroborates an important contribution of miR-132/212 and corresponding target mRNAs to the pathogenesis of AD.

1. INTRODUCTION

Late-onset sporadic Alzheimer's disease (AD), a genetically complex multi-factorial neurodegenerative disease, is the most common form of dementia affecting millions of people worldwide. Although recent genome wide association studies and meta-analysis identified a considerable number of susceptibility gene variants for sporadic late-onset AD, there is still insufficient knowledge concerning the nature of genetic and epigenetic mechanisms that trigger the mechanisms ultimately leading to cell death and neurodegeneration. With the advance of new technologies, however, recent research turned towards the exploration of epigenetic mechanisms such as histone modification and DNA-methylation/-hydroxymethylation as well as non-coding RNA associated gene silencing (Fischer, 2014).

MicroRNAs (miRNA, ~18-25 nucleotides), the largest family of small non-coding RNAs, enable a tightly balanced modulation of gene-expression at the post-transcriptional level. This regulation largely depends on the grade of sequence complementarity between miRNAs and corresponding mRNA targets. In principle, one particular miRNA regulates multiple mRNAs and one specific mRNA is regulated by several miRNAs (BARTEL, 2004). Thus, dysregulation of one miRNA can cause alterations of several different cellular and developmental processes and contribute to the development of a variety of diseases. Interestingly, some miRNAs have also been described in AD (Lau et al., 2014; Satoh, 2012). For example, miR-107 as well as miR-29b target beta-site APP cleaving enzyme 1 (BACE1), an essential protease involved in the amyloidogenic processing of APP as observed in brains of AD patients (Hébert et al., 2008; Nelson and Wang, 2010) and miR-16 was shown to inhibit APP expression in mice (Liu et al., 2012). In addition, miR-132 was reported to play a key role in tau-metabolism, as it regulates exon splicing of tau (Hébert et al., 2012), co-localizes with hyper-phosphorylated tau and negatively correlates with NFT bearing neurons from cortical tissue (Lau et al., 2013).

In this study, we analyzed expression patterns of more than 1 200 miRNAs in the temporal cortex (TC) of 64 samples, including 39 AD and 25 control brains. Two miRNAs, to hsa-miR-132-3p (MIMAT0000426) and hsa-miR-212-3p (MIMAT0000269) showed a genome wide significant downregulation in AD as compared to control brain. Downregulation was verified in additional brain regions and an independent sample. To delineate the primary source of altered miRNA expression signals we further analyzed grey and white matter brain material separately and assessed associations with disease progression. We also examined genome wide mRNA expression to identify likely target genes of miR-132/212.

2. MATERIALS AND METHODS

2.1. Samples

2.1.1. Human brain samples and ethics statement

The initial miRNA screen was carried out in temporal cortex of 64 fresh frozen post-mortem human brain samples provided by the Brain Bank Munich, Germany (MUC cohort). Temporal (TC) and prefrontal cortex (PFC) of eight age and gender matched AD and control pairs selected from MUC cohort were used for validation experiment (MUC validation set). Additionally, we obtained fresh frozen post-mortem PFC from a second sample set containing 225 AD samples and 87 cognitively healthy controls provided by The Netherland Brain Bank (NBB validation set) for independent validation. From the latter cohort, eight age-matched female AD and control pairs were selected for grey and white matter separation (NBB grey/white matter set). Complete sample characteristics are summarized in **Table 1** and **Table S1**. AD patients have been clinically diagnosed according to the NINCDS-ADRDA criteria (McKhann et al., 1984). Human brain tissues provided by Brain Bank Munich (Center for Neuropathology and Prion Research LMU, Munich; coordinating the European brain tissue bank (BNE) and the German national brain tissue bank (BrainNet)) or by The Netherland Brain Bank (Netherlands Institute for Neuroscience, Amsterdam) have been collected from donors for or from whom a written informed consent for a brain autopsy and the use of the material and clinical information for research purposes had been obtained.

2.2. Experimental procedures

2.2.1. Total RNA extraction

Total RNA (>18nt) was extracted from human brain tissue using miRNeasy Mini Kit (Qiagen) according to manufacturer's protocol including on-column DNA digestion with RNase free DNase Set (Qiagen). In brief, we homogenized 50-100mg tissue in 700µl QIAzol (Qiagen) and eluted total RNA within 30µl RNase-free water. Observed RNA integrity numbers for the samples were in the expected range according to literature (Lukiw et al., 2012).

2.2.2. Genome wide miRNA expression profiling

Total RNA (500ng) from TC of MUC cohort was hybridized to microfluid biochip Geniom Biochip Homo sapiens h_v16 plus, (febit biomed GmbH, Heidelberg, Germany) according to manufacturer's protocol. The microarray covered more than 1 200 mature microRNA sequences as annotated in Sanger

miRBase 16 (www.mirbase.org) (Griffiths-Jones et al., 2006) and several additional proprietary human miRNA sequences that had been discovered by deep sequencing. Signal intensities were measured using Geniom RT Analyzer (febit biomed GmbH, Heidelberg, Germany) employing microfluid based enzymatic primer extension assay technique (MPEA) as described elsewhere (Vorwerk et al., 2008). After background correction signal intensity values were calculated for each of the miRNAs over their intra-array replicates. Quantile normalization was applied to correct for inter-array variation. Median signal intensity was calculated for each of the miRNAs over grouped samples (AD vs. control). miRNAs with signal intensity <50 in both groups were considered as not expressed and were excluded from further statistical analysis. Student's T-test was executed on $\log_2$ transformed median signal intensities to identify differently expressed miRNAs of AD versus control samples. To correct for multiple testing, a threshold of 8.16×10^{-05} was set for significant p-values (Bonferroni correction for 613 miRNAs in the analysis). For three biological and technical replicates total RNA was extracted two times from the same tissue and R^2 was calculated using least squared model. All statistical analyses and graphical presentations were accomplished using R (R Development Core Team, 2011).

2.2.3. Semi-quantitative real-time PCR (sqPCR)

Reverse Transcription (RT-PCR) was performed with TaqMan®MicroRNA Reverse Transcription Kit (Applied Biosystems) and specific RT-Primers for TaqMan assays (Applied Biosystems) according to manufacturer's protocol using 10ng total RNA (>18nt) per cDNA reaction. Semi-quantitative real-time PCR was carried out using FAM labeled TaqMan® Assays (Assay IDs: mature hsa-miR132 - 000457, mature hsa-miR-212 - 000515 and RNU48 - 001006) and TaqMan® 2x Universal PCR Mastermix No AmpErase UNG (Applied Biosystems) as described in manufacturer's protocol using maximum amount of cDNA (1.33µl) in 20µl reaction volume. Reactions were measured in technical duplicates on the 7500 Fast System (Applied Biosystems) using SDS software v1.3.1 (Applied Biosystems). Cycle thresholds for duplicates were averaged, normalized against RNU48 average Ct-values and p-values were calculated using student's T-test. RNU48 was experimentally determined as the most stable normalizer among three tested candidate genes. Fold changes were calculated by the use of "delta-delta Ct method" (Livak and Schmittgen, 2001).

2.2.4. Genome wide mRNA expression profiling

Total RNA (500ng) from TC of MUC cohort was amplified and labelled with biotin using Ambion® Illumina® TotalPrep™ RNA Amplification Kit (Ambion) according to manufacturer's protocol. cRNA was eluted in 50µl nuclease-free water and precipitated using ammonium acetate (NH_4OAc) when concentration was <150ng/µl. Direct hybridization of 750ng biotin labelled cRNA to Illumina® Sentrix BeadChips HumanHT-12 v4 (Illumina) was conducted according to manufacturer's protocol. Whole-genome gene expression analysis incorporated 47 231 markers per sample including coding as well as non-coding transcripts based on Human RefSeq 38 (NCBI RefSeq database) and supplementary UniGene content. Processed BeadChips were scanned with Illumina's HiScan. First quality check, background subtraction and quantile normalization were executed with GenomeBead Studio Module for gene expression. Markers with a detection p-value≥0.05 were considered as no-call. Call rates for each marker were calculated separately in both groups (AD vs. control). Markers with a call rate <90% in both groups were considered as non-informative and were excluded from further statistical analysis. Signal intensities were $\log_2$ transformed and student's T-test was carried out to identify differentially expressed markers. To correct for multiple testing, a threshold of 4.4×10^{-06} was set for significant p-values (Bonferroni correction for 11 264 Illumina markers corresponding to 7 421 genes in the analysis). All statistical analyses and graphical presentations were accomplished using R (R Development Core Team, 2011).

2.2.5. Correlation and binding site analyses of mRNA and miRNA

To test the correlation of differentially expressed mRNAs with miR-132/212 expression, signal intensities of mRNA and miRNA were both $\log_2$ transformed before linear regression analysis. To correct for multiple testing, p-value threshold was set to $5x10^{-03}$ (Bonferroni correction of ten markers in the analysis). All statistical analyses were performed using R (R Development Core Team, 2011).

To identify potential miRNA targets or miRNA binding sites we used miRWalk (Dweep et al., 2011) (www.umm.uni-heidelberg.de/apps/zmf/mirwalk/index.html) online target prediction tool. RNA-RNA interaction analysis of mature miRNA sequences to sequences of genome wide significant mRNA transcripts **(Mat S1)**, were performed using online alignment tool RNAhybrid (Krüger and Rehmsmeier, 2006; Rehmsmeier et al., 2004) (http://bibiserv.techfak.uni-bielefeld.de/rnahybrid/submission.html).

3. RESULTS

3.1. Downregulation of miR-132/212 cluster in temporal cortex of AD patients

We explored genome wide miRNA expression profiles in the temporal cortex of 39 AD patients and 25 controls obtained from the Brain Bank Munich **(Table 1)**. By hybridizing total RNA to a Febit Geniom Biochip utilizing MPEA-technique (Vorwerk et al., 2008), signal intensities of 1 221 mature miRNAs annotated in miRBase release 16 (www.mirbase.org) were examined **(Figure S1)**. Biological and technical replicates were included as internal quality controls and were found to be highly correlated to each other (R^2>0.89). After filtering for non-expressed and non-informative miRNAs, 613 miRNAs remained for further statistical analysis. Age and gender were tested as covariates in logistic regression models but no significant effects were observed (data not shown). We further applied student's T-test on log_2 transformed signal intensities resulting in 102 miRNAs that exceeded unadjusted p-values<0.05 **(Table 2)**. From these, 41 miRNAs showed increased and 61 showed decreased expression levels in AD samples. When comparing our results (N=102 miRNAs) with published miRNAs (N=323 miRNAs) for which dysregulation in AD has been described (Lau et al., 2014; Satoh, 2012), we observed an overlap for 27 miRNAs with 14 showing deregulation in the same direction as previously described **(Table 2).**

Two miRNAs, hsa-miR-132-3p (MIMAT0000426) and hsa-miR-212-3p (MIMAT0000269), showed genome wide significance ($p_{hsa\text{-}miR\text{-}132\text{-}3p}=5.02x10^{-07}$; $p_{hsa\text{-}miR\text{-}212\text{-}3p}=2.38x10^{-06}$) and passed Bonferroni correction (p-values<$8.16x10^{-05}$). In general, hsa-miR-132-3p shows higher expression levels than hsa-miR-212-3p. Both have recently been related to AD by several groups **(Table 2)** (Cogswell et al., 2008; Lau et al., 2013; Wang et al., 2011). We observed a rather homogeneous pattern of downregulation of almost 60% in AD as compared to controls for both miRNAs ($fold_{hsa\text{-}miR\text{-}132\text{-}3p}=0.407$; $fold_{hsa\text{-}miR\text{-}212\text{-}3p}=0.409$; **Figure 1 A-B**). Further, we explored a potential association of miRNA expression levels with Braak stages **(Figure 1 C-D)**. Using linear regression analysis, we observed a significant decline of expression with advancing Braak stage ($p_{hsa\text{-}miR\text{-}132\text{-}3p}=3.86x10^{-08}$; $p_{hsa\text{-}miR\text{-}212\text{-}3p}=1.13x10^{-05}$).

3.2. Verification of hsa-miR-132-3p and hsa-miR-212-3p expression levels

To validate our results, we applied semi-quantitative real-time PCR (sqPCR) using different sample sets **(Table 1, Table S1)**. Expression patterns were (i) re-analyzed in eight age and gender matched sample pairs from TC (MUC validation set), (ii) investigated in a second brain region (PFC) of the

same samples (MUC validation set), and (iii) validated in PFC of an independent cohort (225 AD, 87 controls) obtained from Netherland Brain Bank (NBB validation set).

For all sample sets we observed higher dCt-values indicating a consistent downregulation of both mature miRNAs in AD as compared to controls (MUC validation set TC: $p_{hsa\text{-}miR\text{-}132\text{-}3p}=2.68x10^{-03}$; $p_{hsa\text{-}miR\text{-}212\text{-}3p}=1.81x10^{-02}$; PFC: $p_{hsa\text{-}miR\text{-}132\text{-}3p}=4.80x10^{-02}$; $p_{hsa\text{-}miR\text{-}212\text{-}3p}=1.72x10^{-02}$; NBB validation set: $p_{hsa\text{-}miR\text{-}132\text{-}3p}=5.43x10^{-18}$; $p_{hsa\text{-}miR\text{-}212\text{-}3p} = 3.53x10^{-18}$; **Figure 2 A-F)**. The expression of both miRNAs was decreased in AD patients as compared to controls by approximately 45 - 65 % (hsa-miR-132-3p: $fold_{TC\_MUC}=0.347$, $fold_{PFC\_MUC}=0.548$, $fold_{PFC\_NBB}=0.413$; hsa-miR-212-3p: $fold_{TC\_MUC}=0.476$, $fold_{PFC\_MUC}=0.513$, $fold_{PFC\_NBB}=0.391$) with hsa-miR-132-3p showing higher expression levels than hsa-miR-212-3p. Finally, combining all data sets showed a very robust downregulation of both miRNAs by almost 65% (hsa-miR-132-3p: $p=4.86x10^{-20}$, fold=0.371; hsa-miR-212-3p: $p=2.38x10^{-20}$, fold=0.356).

3.3. hsa-miR-132-3p and hsa-miR-212-3p are strongly downregulated in grey matter

To further delineate the origin of decreased expression, we dissected grey and white matter sections from PFC of eight age matched pairs of female NBB samples and repeated miRNA expression analysis using sqPCR. hsa-miR-132-3p and hsa-miR-212-3p were significantly downregulated in grey as well as in white matter preparations of AD samples compared to controls. However, the differences identified in white matter samples were much weaker (hsa-miR-132-3p: $p=2.40x10^{-02}$, fold=0.633; hsa-miR-212-3p: $p=4.31x10^{-02}$, fold=0.648) than expression alterations observed in grey matter preparations (hsa-miR-132-3p: $p=9.41x10^{-04}$, fold=0.429; hsa-miR-212-3p: $p=2.67x10^{-03}$, fold=0.395) **(Figure 2 G-J)**. Our results indicate a stronger downregulation of miR-132/212 in grey matter sections, which compared to white matter contain a higher proportion of neurons and dendrites.

3.4. Expression levels of neuronal-enriched miRNAs and miR-132/212 in Braak stages 0-VI

Since the observed downregulation in AD might be a result of advancing neuronal degradation during disease progression, we compared the expression levels of miR-132/212 together with other previously identified neuronal-enriched miRNAs (Lau et al., 2013) using our microarray data set for TC of the MUC cohort. Across all Braak stages 0-VI we observed a considerable stronger downregulation for hsa-miR-132 and hsa-miR-212 compared to the other neuronal-enriched miRNAs starting already at Braak stage II **(Figure S2)**.

3.5. Gene Expression alterations in temporal cortex of AD and control samples

We next performed mRNA expression analysis in 64 TC samples of the MUC cohort utilizing Illumina sentrix bead arrays. After normalization and filtering we applied student's T-test on the $\log_2$ signal intensities of 11 264 remaining markers. In total, 3 544 markers corresponding to 3 270 genes were found to be differentially expressed between AD and control samples (p-values<0.05) **(Table S2)**. Interestingly, we identified 9 down- and 10 upregulated mRNAs in our dataset from 47 genes that have previously been reported to be regulated by hsa-miR-132-3p and/or hsa-miR-212-3p **(Table S2)** (Lau et al., 2014; Wanet et al., 2012).

Ten markers corresponding to ten individual genes remained at a genome wide significant level ($p<4.4x10^{-06}$) after applying a Bonferroni correction for multiple testing **(Table 3)**. The strongest alterations were observed for three small nuclear RNAs, RNU1G2 ($p=1.51x10^{-09}$), RNU1-3 ($p=4.37x10^{-09}$), and RNU1-5 ($p=1.55x10^{-08}$) followed by adipocyte enhancer binding protein 1 (AEBP1; $p=9.74x10^{-08}$), nuclear factor of kappa light polypeptide gene enhancer in B-cells 1 (NFKB1; $p=1.44x10^{-07}$), proteinkinase 2 (PKN2; $p=6.34x10^{-07}$), HMG box transcription factor 1 (HBP1; $p=7.51x10^{-07}$), CREB3 regulatory factor (C5ORF41; $p=8.90x10^{-07}$) and glial fibrillary acidic protein (GFAP; $p=3.70x10^{-06}$). These genes were upregulated in AD whereas tetraspanin 7 (TSPAN7; $p=3.32x10^{-06}$) was significantly downregulated in AD **(Figure S3)**.

3.6. Correlations between miRNA and mRNA expression

Since miRNAs are known to mediate gene regulatory effects we next examined correlations between miR-132/212 and the ten differentially expressed transcripts identified in the TC samples from MUC cohort. As demonstrated in **Table 3**, strong correlations between expression levels of these ten mRNAs and the two miRNAs hsa-miR-132-3p and hsa-miR-212-3p were observed by linear regression **(Figure S4)**. Correlations for GFAP, AEBP1 and TSPAN7 even exceeded genome wide significance for both miRNAs. Given these strong correlations between miRNA and mRNA expression levels we screened these genes for potential miR-132/212 binding sites using online prediction tools. Binding sites for both miRNAs were predicted in PKN2, C5ORF41 and GFAP, and a binding site for hsa-miR-132-3p was predicted for NFKB1 according to miRWalk (Dweep et al., 2011), a bioinformatics tool combining several prediction tools by comparative analysis. Additionally, we analyzed potential RNA-RNA interactions of the 3'UTR of the transcript corresponding to the appropriate Illumina Marker for each of these four mRNAs to mature miRNA sequences using

RNAHybrid (Krüger and Rehmsmeier, 2006; Rehmsmeier et al., 2004), an online available alignment tool. The target/miRNA concatenation with the best minimum free energy (mfe) is presented in supplementary **Figure S5**. Together, we identified potential binding sites of hsa-miR-132-3p and/or hsa-miR-212-3p on four of ten dysregulated mRNAs identified in TC of in AD patients by *in silico* analysis.

4. DISCUSSION

Using a microarray-based miRNome-wide screening we observed 102 deregulated miRNAs in temporal cortical brain regions of AD patients compared to controls including two miRNAs, hsa-miR-132-3p and hsa-miR-212-3p showing alterations exceeding the level of genome wide significance. Remarkably, deregulations of a considerable number (~25%) of these 102 miRNAs have already been described in AD (Lau et al., 2014; Satoh, 2012). However, these previous studies show rather inconsistencies regarding types and expression patterns of the miRNAs identified. Possible reasons may include considerable differences regarding sample sizes, brain regions and technical methodologies, which have been applied. A recent analysis by Kolbert *et al*. comparing different platforms and technologies demonstrated considerable differences in miRNA transcript detection ranging from 35% up to 70% as well as differences in expression intensities across the tested methodologies (Kolbert et al., 2013). As such, these methodological issues are most likely to explain the discrepancies in miRNA expression patterns observed in AD so far, at least for miRNAs showing weak to intermediate alterations of expression patterns.

We observed genome wide significant downregulation of the miR-132/212 cluster in AD, which was confirmed by sqPCR in temporal and prefrontal cortex of the same individuals, and in PFC of an independent, larger sample set from the Netherland Brain Bank (NBB). It has to be mentioned that the NBB samples are partially overlapping with those used in a previous study by Lau *et al* 2013, who also observed downregulation for hsa-miR-132-3p. However, in contrast to our study Lau *et al* used the NanoString technology and analyzed dissected grey matter samples from the hippocampus and prefrontal cortex.

In addition, downregulation of miR-132 and miR-212 has been described for several brain regions in AD, as well as in cellular and mouse models for AD (Cogswell et al., 2008; Hébert et al., 2013; Lau et al., 2013; Wang et al., 2011; Wong et al., 2013). The miR-132/212 cluster is processed from a joint primary transcript encoded by an intergenic region on chromosome 17. Our results indicate higher expression levels and stronger downregulation for hsa-miR-132-3p compared to hsa-miR-212-3p, which is in line with literature and might be explained by post-transcriptional regulation (Magill et al., 2010; Wanet et al., 2012).

We observed a consistent downregulation of the miR-132/212 cluster already at early stages of AD (Braak stage III-IV) with an advancing decline during disease progression (Braak stage>IV) in temporal cortex (MUC cohort). Comparing these results with expression levels of other described

neuronal-enriched miRNAs revealed that downregulation of miR-132/212 appears already at very early stages of AD and more pronounced compared to others and thus seems to be independent from advancing loss of neurons. These observations are in line with previous findings in PFC and thereby corroborates its crucial implication in disease aetiology rather than being merely a secondary effect due to neuronal loss (Lau et al., 2013). To further explore the cellular origin of the observed downregulation, we separated white and grey matter sections and detected a considerable stronger downregulation of both miRNAs in grey matter of AD samples (female), which supports the primarily neuronal origin of the observed miR-132/212 dysregulation. In contrast to our results, Wang *et al* (Wang et al., 2011) reported a downregulation of miR-212 in white matter rather than grey matter regions. This discrepancy might derive from the rather small sample size (N=10) of their study in combination with the applied gender stratification. Corresponding to our study, Lau *et al* (Lau et al., 2013) observed a clear decrease of miR-132 expression especially in tangle bearing cortical neurons of AD patients. In addition, further studies showed that the loss of miR-132 affects the processing of *MAPT* and leads to aberrant splicing of *MAPT* exon 10 in frontotemporal dementia and progressive supranuclear palsy mediated by PTBP2 (Hébert et al., 2012; Lau et al., 2014; Smith et al., 2011). Furthermore, miR-132 has been linked to several pathways playing a major role in the pathogenesis of AD, such as inflammatory processes (Soreq and Wolf, 2011), synaptic function, -structure and -plasticity (Bicker et al., 2014; Edbauer et al., 2010; Remenyi et al., 2013), and cholinergic signaling by targeting AChE (Lu et al., 2013; Shaked et al., 2009; Shaltiel et al., 2013). Both miRNAs (miR-132 and miR-212) are also involved in neuronal migration, axonal growth and neuronal morphology (Hancock et al., 2014; Magill et al., 2010) and decreased expression of miR-132 is associated with the induction of apoptosis via de-repression of FOXO3a (Wong et al., 2013).

So far, only few validated target genes of miR-132 and miR-212 have been described (Lau et al., 2014; Wanet et al., 2012). Interestingly, several of these known targets, such as SIRT1, FOXO1, and p250GAP also showed a deregulation in our mRNA expression analysis in AD (**Table S2)**. So far, just one group performed simultaneous miRNA and mRNA expression analyses using a limited number of eight AD and control brains, each (Nunez-Iglesias et al., 2010). In this study, we present joint genome wide miRNA and mRNA expression profiles in temporal cortex of a much larger sample set (64 samples). Interestingly, among the strongest deregulated mRNAs identified in this study, were a considerable number of genes that have previously been associated with AD. For example, we identified a strong upregulation of three small nuclear RNAs, RNU1-3, RNU1-5 and RNU1G2 that are

part of the cellular spliceosome complex. These small nuclear RNAs have recently been described to form tangle-like structures, aggregate with NFTs and to severely affect splicing processes in AD (Bai et al., 2013; Hales et al., 2014). Moreover, GFAP and NFkB1, two well-known markers of inflammation in AD, were strongly upregulated in brains of AD patients (Ascolani et al., 2012; Huang et al., 2005; Ingelsson et al., 2004; Nagele et al., 2004).

We also explored possible miR-132/212 binding sites at 3'UTRs of those mRNAs showing the strongest expression alterations and identified potential binding sites at four of ten genome wide significant deregulated mRNAs. The results from the miRWalk prediction tool were further supported by energetically most reasonable miRNA-RNA structures. The binding site prediction and strong associations with the glial derived inflammatory genes, GFAP and NFkB1 (Ingelsson et al., 2004; Lian et al., 2014) is somewhat surprising as our results indicate a primarily neuronal origin of the miR-132/212 decrease. However the fact that downregulation of miR-132/212 also occurred in white-matter fractions with a larger content of glial cells and the usage of whole-brain material for gene expression analyses may explain these findings.

Concerning the other target genes PKN2 and C5ORF41, both are expressed in neurons. Functionally PKN2, a protein kinase, was found to promote neurite growth in hippocampal neurons (Buchser et al., 2010) and C5ORF41 to degrade CREB3, which is implicated in numerous functions such as unfolded protein response during ER stress, viral infections and immunity (Audas et al., 2008; Yang et al., 2013). Interestingly, transcription of the miR-132/212 locus is regulated by CREB another member of the CREB family (Wanet et al., 2012). Likewise to AD loss of CREB as well as miR-132/212 cause a decrease of dendritic growth, branching of neurons and disturbances of memory formation (Hernandez-Rapp et al., 2015; Magill et al., 2010).

Since many of the target genes mentioned above are associated with cellular or clinical alterations typically occurring in AD, it may be hypothesized that following-up these *in silico* results may provide us with a better understanding of biological mechanisms leading to AD.

In conclusion, our study adds substantial evidence to an early and major involvement of hsa-miR-132-3p and hsa-miR-212-3p in the pathogenesis of AD and further supports the primarily neuronal origin of these miRNAs. In addition, we provide for the first time a large data set of genome wide miRNA and mRNA expression profiles from AD and control brains highlighting some new potential miR-132/212 target genes. Further functional work, however is mandatory to fully understand the cellular and

biological consequences of the downregulated miRNAs and to characterize and validate potential target genes contributing to AD.

ACKNOWLEDGEMENTS

The authors are grateful to all individuals and their families who participated in this study for their contribution. We would like to thank the Brain Bank Munich (Center for Neuropathology and Prion Research LMU, Munich; coordinating the European brain tissue bank (BNE) and the German national brain tissue bank (BrainNet)) and Netherland Brain Bank (Netherlands Institute for Neuroscience, Amsterdam) for providing the brain tissues. This work was supported by the German Federal Ministry of Education and Research (BMBF) National Genome Research Network (NGFN) grant No. 01GS08125 to MR and through the Helmholtz Alliance for Mental Health in an Aging Society (HELMA) Grant No. Ha-15 to MR. HH is supported by the AXA Research Fund, the "Fondation Université Pierre et Marie Curie" and the "Fondation pour la Recherche sur Alzheimer", Paris, France. The research leading to these results has received funding from the program "Investissements d'avenir" ANR-10-IAIHU-06.

DISCLOSURE STATEMENT

The authors declare that there are no conflicts of interest and no competing financial interests.

SUPPLEMENTARY INFORMATION (SI)

Supplementary information is available at *Neurobiology of Aging's* website.

LITERATURE

Ascolani, A., Balestrieri, E., Minutolo, A., Mosti, S., Spalletta, G., Bramanti, P., Mastino, A., Caltagirone, C., Macchi, B., 2012. Dysregulated NF-κB pathway in peripheral mononuclear cells of Alzheimer's disease patients. Curr. Alzheimer Res. 9, 128–37. doi:10.2174/156720512799015091

Audas, T.E., Li, Y., Liang, G., Lu, R., 2008. A novel protein, Luman/CREB3 recruitment factor, inhibits Luman activation of the unfolded protein response. Mol. Cell. Biol. 28, 3952–66. doi:10.1128/MCB.01439-07

Bai, B., Hales, C.M., Chen, P., Gozal, Y., Dammer, E.B., Fritz, J.J., 2013. U1 small nuclear ribonucleoprotein complex and RNA splicing alterations in Alzheimer ' s disease. doi:10.1073/pnas.1310249110/-/DCSupplemental.www.pnas.org/cgi/doi/10.1073/pnas.1310249110

BARTEL, D., 2004. MicroRNAsGenomics, Biogenesis, Mechanism, and Function. Cell 116, 281–297. doi:10.1016/S0092-8674(04)00045-5

Bicker, S., Lackinger, M., Weiß, K., Schratt, G., 2014. MicroRNA-132, -134, and -138: a microRNA troika rules in neuronal dendrites. Cell. Mol. Life Sci. doi:10.1007/s00018-014-1671-7

Buchser, W.J., Slepak, T.I., Gutierrez-Arenas, O., Bixby, J.L., Lemmon, V.P., 2010. Kinase/phosphatase overexpression reveals pathways regulating hippocampal neuron morphology. Mol. Syst. Biol. 6, 391. doi:10.1038/msb.2010.52

Cogswell, J.P., Ward, J., Taylor, I.A., Waters, M., Shi, Y., Cannon, B., Kelnar, K., Kemppainen, J., Brown, D., Chen, C., Prinjha, R.K., Richardson, J.C., Saunders, A.M., Roses, A.D., Richards, C.A., 2008. Identification of miRNA changes in Alzheimer's disease brain and CSF yields putative biomarkers and insights into disease pathways. J. Alzheimers. Dis. 14, 27–41.

Dweep, H., Sticht, C., Pandey, P., Gretz, N., 2011. miRWalk--database: prediction of possible miRNA binding sites by "walking" the genes of three genomes. J. Biomed. Inform. 44, 839–47. doi:10.1016/j.jbi.2011.05.002

Edbauer, D., Neilson, J.R., Foster, K. a, Wang, C.-F., Seeburg, D.P., Batterton, M.N., Tada, T., Dolan, B.M., Sharp, P. a, Sheng, M., 2010. Regulation of synaptic structure and function by FMRP-associated microRNAs miR-125b and miR-132. Neuron 65, 373–84. doi:10.1016/j.neuron.2010.01.005

Fischer, A., 2014. Epigenetic memory: the Lamarckian brain. EMBO J. doi:10.1002/embj.201387637

Griffiths-Jones, S., Grocock, R.J., van Dongen, S., Bateman, A., Enright, A.J., 2006. miRBase: microRNA sequences, targets and gene nomenclature. Nucleic Acids Res. 34, D140–4. doi:10.1093/nar/gkj112

Hales, C.M., Dammer, E.B., Diner, I., Yi, H., Seyfried, N.T., Gearing, M., Glass, J.D., Montine, T.J., Levey, A.I., Lah, J.J., 2014. Aggregates of small nuclear ribonucleic acids (snRNAs) in Alzheimer's disease. Brain Pathol. doi:10.1111/bpa.12133

Hancock, M.L., Preitner, N., Quan, J., Flanagan, J.G., 2014. MicroRNA-132 Is Enriched in Developing Axons, Locally Regulates Rasa1 mRNA, and Promotes Axon Extension. J. Neurosci. 34, 66–78. doi:10.1523/JNEUROSCI.3371-13.2014

Hébert, S.S., Horré, K., Nicolaï, L., Papadopoulou, A.S., Mandemakers, W., Silahtaroglu, A.N., Kauppinen, S., Delacourte, A., De Strooper, B., 2008. Loss of microRNA cluster miR-29a/b-1 in sporadic Alzheimer's disease correlates with increased BACE1/beta-secretase expression. Proc. Natl. Acad. Sci. U. S. A. 105, 6415–20. doi:10.1073/pnas.0710263105

Hébert, S.S., Sergeant, N., Buée, L., 2012. MicroRNAs and the Regulation of Tau Metabolism. Int. J. Alzheimers. Dis. 2012, 406561. doi:10.1155/2012/406561

Hébert, S.S., Wang, W.-X., Zhu, Q., Nelson, P.T., 2013. A study of small RNAs from cerebral neocortex of pathology-verified Alzheimer's disease, dementia with lewy bodies, hippocampal sclerosis, frontotemporal lobar dementia, and non-demented human controls. J. Alzheimers. Dis. 35, 335–48. doi:10.3233/JAD-122350

Hernandez-Rapp, J., Smith, P.Y., Filali, M., Goupil, C., Planel, E., Magill, S.T., Goodman, R.H., Hébert, S.S., 2015. Memory formation and retention are affected in adult miR-132/212 knockout mice. Behav. Brain Res. 287, 15–26. doi:10.1016/j.bbr.2015.03.032

Huang, Y., Liu, F., Grundke-Iqbal, I., Iqbal, K., Gong, C.-X., 2005. NF-kappaB precursor, p105, and NF-kappaB inhibitor, IkappaBgamma, are both elevated in Alzheimer disease brain. Neurosci. Lett. 373, 115–8. doi:10.1016/j.neulet.2004.09.074

Ingelsson, M., Fukumoto, H., Newell, K.L., Growdon, J.H., Hedley-Whyte, E.T., Frosch, M.P., Albert, M.S., Hyman, B.T., Irizarry, M.C., 2004. Early A accumulation and progressive synaptic loss, gliosis, and tangle formation in AD brain. Neurology 62, 925–931. doi:10.1212/01.WNL.0000115115.98960.37

Kolbert, C.P., Feddersen, R.M., Rakhshan, F., Grill, D.E., Simon, G., Middha, S., Jang, J.S., Simon, V., Schultz, D.A., Zschunke, M., Lingle, W., Carr, J.M., Thompson, E.A., Oberg, A.L., Eckloff, B.W., Wieben, E.D., Li, P., Yang, P., Jen, J., 2013. Multi-Platform Analysis of MicroRNA Expression Measurements in RNA from Fresh Frozen and FFPE Tissues 8. doi:10.1371/journal.pone.0052517

Krüger, J., Rehmsmeier, M., 2006. RNAhybrid: microRNA target prediction easy, fast and flexible. Nucleic Acids Res. 34, W451–4. doi:10.1093/nar/gkl243

Lau, P., Bossers, K., Janky, R., Salta, E., Frigerio, C.S., Barbash, S., Rothman, R., Sierksma, A.S.R., Thathiah, A., Greenberg, D., Papadopoulou, A.S., Achsel, T., Ayoubi, T., Soreq, H., Verhaagen, J., Swaab, D.F., Aerts, S., De Strooper, B., 2013. Alteration of the microRNA network during the progression of Alzheimer's disease. EMBO Mol. Med. doi:10.1002/emmm.201201974

Lau, P., Frigerio, C.S., De Strooper, B., 2014. Variance in the identification of microRNAs deregulated in Alzheimer's disease and possible role of lincRNAs in the pathology: the need of larger datasets. Ageing Res. Rev. doi:10.1016/j.arr.2014.02.006

Lian, H., Yang, L., Cole, A., Sun, L., Chiang, A.C.-A., Fowler, S.W., Shim, D.J., Rodriguez-Rivera, J., Taglialatela, G., Jankowsky, J.L., Lu, H.-C., Zheng, H., 2014. NFκB-Activated Astroglial Release of Complement C3 Compromises Neuronal Morphology and Function Associated with Alzheimer's Disease. Neuron 85, 101–115. doi:10.1016/j.neuron.2014.11.018

Liu, W., Liu, C., Zhu, J., Shu, P., Yin, B., Gong, Y., Qiang, B., Yuan, J., Peng, X., 2012. MicroRNA-16 targets amyloid precursor protein to potentially modulate Alzheimer's-associated pathogenesis in SAMP8 mice. Neurobiol. Aging 33, 522–34. doi:10.1016/j.neurobiolaging.2010.04.034

Livak, K.J., Schmittgen, T.D., 2001. Analysis of relative gene expression data using real-time quantitative PCR and the 2(-Delta Delta C(T)) Method. Methods 25, 402–8. doi:10.1006/meth.2001.1262

Lu, L., Zhang, X., Zhang, B., Wu, J., Zhang, X., 2013. Synaptic acetylcholinesterase targeted by microRNA-212 functions as a tumor suppressor in non-small cell lung cancer. Int. J. Biochem. Cell Biol. 45, 2530–2540.

Lukiw, W.J., Andreeva, T. V, Grigorenko, A.P., Rogaev, E.I., 2012. Studying micro RNA Function and Dysfunction in Alzheimer's Disease. Front. Genet. 3, 327. doi:10.3389/fgene.2012.00327

Magill, S.T., Cambronne, X.A., Luikart, B.W., Lioy, D.T., Leighton, B.H., Westbrook, G.L., Mandel, G., Goodman, R.H., 2010. microRNA-132 regulates dendritic growth and arborization of newborn neurons in the adult hippocampus. Proc. Natl. Acad. Sci. U. S. A. 107, 20382–7. doi:10.1073/pnas.1015691107

McKhann, G., Drachman, D., Folstein, M., Katzman, R., Price, D., Stadlan, E.M., 1984. Clinical diagnosis of Alzheimer's disease: report of the NINCDS-ADRDA Work Group under the auspices of Department of Health and Human Services Task Force on Alzheimer's Disease. Neurology 34, 939–44.

Nagele, R.G., Wegiel, J., Venkataraman, V., Imaki, H., Wang, K.-C., Wegiel, J., 2004. Contribution of glial cells to the development of amyloid plaques in Alzheimer's disease. Neurobiol. Aging 25, 663–74. doi:10.1016/j.neurobiolaging.2004.01.007

Nelson, P.T., Wang, W.-X., 2010. MiR-107 is reduced in Alzheimer's disease brain neocortex: validation study. J. Alzheimers. Dis. 21, 75–9. doi:10.3233/JAD-2010-091603

Nunez-Iglesias, J., Liu, C.-C., Morgan, T.E., Finch, C.E., Zhou, X.J., 2010. Joint genome-wide profiling of miRNA and mRNA expression in Alzheimer's disease cortex reveals altered miRNA regulation. PLoS One 5, e8898. doi:10.1371/journal.pone.0008898

R Development Core Team, R., 2011. R: A Language and Environment for Statistical Computing. R Found. Stat. Comput., R Foundation for Statistical Computing. doi:10.1007/978-3-540-74686-7

Rehmsmeier, M., Steffen, P., Hochsmann, M., Giegerich, R., 2004. Fast and effective prediction of microRNA/target duplexes. RNA 10, 1507–17. doi:10.1261/rna.5248604

Remenyi, J., van den Bosch, M.W.M., Palygin, O., Mistry, R.B., McKenzie, C., Macdonald, A., Hutvagner, G., Arthur, J.S.C., Frenguelli, B.G., Pankratov, Y., 2013. miR-132/212 Knockout Mice Reveal Roles for These miRNAs in Regulating Cortical Synaptic Transmission and Plasticity. PLoS One 8, e62509. doi:10.1371/journal.pone.0062509

Satoh, J., 2012. Molecular network of microRNA targets in Alzheimer's disease brains. Exp. Neurol. 235, 436–46. doi:10.1016/j.expneurol.2011.09.003

Satoh, J., 2010. MicroRNAs and their therapeutic potential for human diseases: aberrant microRNA expression in Alzheimer's disease brains. J. Pharmacol. Sci. 114, 269–75.

Shaked, I., Meerson, A., Wolf, Y., Avni, R., Greenberg, D., Gilboa-Geffen, A., Soreq, H., 2009. MicroRNA-132 potentiates cholinergic anti-inflammatory signaling by targeting acetylcholinesterase. Immunity 31, 965–73. doi:10.1016/j.immuni.2009.09.019

Shaltiel, G., Hanan, M., Wolf, Y., Barbash, S., Kovalev, E., Shoham, S., Soreq, H., 2013. Hippocampal microRNA-132 mediates stress-inducible cognitive deficits through its acetylcholinesterase target. Brain Struct. Funct. 218, 59–72. doi:10.1007/s00429-011-0376-z

Smith, P.Y., Delay, C., Girard, J., Papon, M.-A., Planel, E., Sergeant, N., Buée, L., Hébert, S.S., 2011. MicroRNA-132 loss is associated with tau exon 10 inclusion in progressive supranuclear palsy. Hum. Mol. Genet. 20, 4016–24. doi:10.1093/hmg/ddr330

Soreq, H., Wolf, Y., 2011. NeurimmiRs: microRNAs in the neuroimmune interface. Trends Mol. Med. 17, 548–55. doi:10.1016/j.molmed.2011.06.009

Vorwerk, S., Ganter, K., Cheng, Y., Hoheisel, J., Stähler, P.F., Beier, M., 2008. Microfluidic-based enzymatic on-chip labeling of miRNAs. N. Biotechnol. 25, 142–149. doi:10.1016/j.nbt.2008.08.005

Wanet, A., Tacheny, A., Arnould, T., Renard, P., 2012. miR-212/132 expression and functions: within and beyond the neuronal compartment. Nucleic Acids Res. 40, 4742–53. doi:10.1093/nar/gks151

Wang, W.-X., Huang, Q., Hu, Y., Stromberg, A.J., Nelson, P.T., 2011. Patterns of microRNA expression in normal and early Alzheimer's disease human temporal cortex: white matter versus gray matter. Acta Neuropathol. 121, 193–205. doi:10.1007/s00401-010-0756-0

Wong, H.-K.A., Veremeyko, T., Patel, N., Lemere, C.A., Walsh, D.M., Esau, C., Vanderburg, C., Krichevsky, A.M., 2013. De-repression of FOXO3a death axis by microRNA-132 and -212 causes neuronal apoptosis in Alzheimer's disease. Hum. Mol. Genet. ddt164–. doi:10.1093/hmg/ddt164

Yang, Y., Jin, Y., Martyn, A.C., Lin, P., Song, Y., Chen, F., Hu, L., Cui, C., Li, X., Li, Q., Lu, R., Wang, A., 2013. Expression pattern implicates a potential role for luman recruitment factor in the process of implantation in uteri and development of preimplantation embryos in mice. J. Reprod. Dev. 59, 245–51.

FIGURES

Figure 1: miRNA expression levels of significantly deregulated miRNAs in TC of MUC cohort based on microarray data

Distribution of log_2 transformed signal intensities of (A) hsa-miR-132-3p and (B) hsa-miR-212-3p in 64 analyzed human temporal cortices. Both miRNAs showed ~ 60 % downregulation in AD patients compared to healthy controls ($p\text{-Value}_{hsa\text{-}miR\text{-}132\text{-}3p} = 5.02x10^{-07}$; $p\text{-Value}_{hsa\text{-}miR\text{-}212\text{-}3p} = 2.38x10^{-06}$). Graphical illustration depicts significant associations between (C) hsa-miR-132-3p (p-value = $3.86x10^{-08}$, $R^2 = 0.40$) as well as (D) hsa-miR-212-3p (p-value = $1.13x10^{-05}$, $R^2 = 0.28$) expression levels and Braak stages in TC of 64 analyzed samples from MUC cohort; p-values and R^2 were calculated by linear regression analysis using R.

Figure 2: Distribution of miRNA expression data examined by semi-quantitative PCR

dCt-values of indicated miRNAs measured in TC (A, B) and PFC (C, D) of age and gender matched MUC samples as well as in PFC of NBB samples (E, F) and in age and gender matched white (G, H) and grey matter (I, J) separated PFC of NBB samples. Graphic illustrates significant downregulation of both analyzed miRNAs (A, C, E, G, I: hsa-miR-132-3p, B, D, F, H, J: hsa-miR-212-3p) in AD as compared to control samples (A-F) and in grey matter of AD patients as compared to white matter AD samples (G-J). dCt-values were normalized against RNU48 and p-values were calculated either by paired (A-D) or unpaired (E-J) one-sided student's T-test confirming results from miRNA expression profiling.

TABLES

Table 1: Sample characteristics

General information on post-mortem human brain samples analyzed in the present study

cohort	samples	N =	age (mean ± SD) [years]	post-mortem delay (mean ± SD) [hours]	Braak stage (mean ± SD)	APOEε4 carrier [%]	tissue	experiment
MUC cohort	**AD**	39	80.4 ± 8.2	30.2 ± 16.6	5 ± 1	64.1	temporal cortex	genome wide miRNA (febit MPEA microarray h_v16plus, mirBase16) and genome wide mRNA expression profile (illumina Sentrix bead arrays HT12v4)
	male	15	78.9 ± 7.4	33.9 ± 17.9	5 ± 1	66.7		
	female	24	81.3 ± 8.7	26.2 ± 14.7	5 ± 0	60.0		
	CTRL	25	65.3 ± 16.9	23.4 ± 10.4	1 ± 1	16.0		
	male	15	59.4 ± 16.7	24.9 ± 10.9	2 ± 1	10.0		
	female	10	74.2 ± 13.3	22.5 ± 10.5	1 ± 1	20.0		
MUC validation set	**AD**	8	78.0 ± 8.3	30.4 ± 15.5	6 ± 0	37.5	temporal cortex and frontal cortex	sqPCR for miR-132 and miR-212 using TaqMan Assays
	male	3	74.3 ± 12.5	38.00 ± 17	6 ± 1	33.3		
	female	5	80.2 ± 5.2	27.40 ± 15.7	6 ± 0	40.0		
	CTRL	8	78.4 ± 8.1	30.4 ± 12.4	2 ± 1	12.5		
	male	3	75.0 ± 12.0	31.0 ± 15.4	2 ± 1	33.3		
	female	5	80.4 ± 5.3	30.0 ± 12.1	3 ± 1	0		
NBB validation set	AD	225	79.4 ± 11.0	5.3 ± 1.4	5 ± 1	66.2	frontal cortex	sqPCR for miR-132 and miR-212 using TaqMan Assays
	male	67	74.4 ± 10.8	5.2 ± 1.3	5 ± 1	70.2		
	female	158	81.5 ± 10.5	5.3 ± 1.5	5 ± 1	64.6		
	CTRL	87	81.8 ± 9.2	6.7 ± 2.0	2 ± 1	24.1		
	male	37	82.1 ± 7.4	7.2 ± 2.2	2 ± 1	21.6		
	female	50	81.7 ± 10.4	6.3 ± 1.8	2 ± 1	26.0		
NBB grey/white matter set[‡]	**AD**	8	84.8 ± 8.4	5.4 ± 1.6	5 ± 1	0	frontal cortex	sqPCR for miR-132 and miR-212 using TaqMan Assays
	male	-	-	-	-	-		
	female	8	84.8 ± 8.4	5.4 ± 1.6	5 ± 1	0		
	CTRL	8	85.1 ± 6.1	6.4 ± 0.7	1 ± 0	0		
	male	-	-	-	-	-		
	female	8	85.1 ± 6.1	6.4 ± 0.7	1 ± 0	0		

[‡] More detailed information about samples in validation sets can be found in supplementary table S1

Table 2: Deregulated miRNAs in temporal cortex of AD patients

log_2 median signal intensities and nominal p-values of 102 deregulated miRNAs identified by miRNA expression screening of 64 human TC samples and their overlap with literature (3; 4; 46). Bold text highlights inconsistent results; nominal p-values marked with (‡) also reached statistical significance after Bonferroni correction for multiple testing (p-value < 8.16×10^{-05}).

miRNA	log_2 median signal intensities		trend in AD	student's T-test p-values	trend in AD in literature
	Ctrl	AD			
hsa-miR-132	11.12	9.82	down	5.02×10^{-07} (‡)	down (Cogswell et al., 2008; Lau et al., 2013)
hsa-miR-212	7.57	6.28	down	2.38×10^{-06} (‡)	down (Cogswell et al., 2008; Wang et al., 2011)
hsa-miR-423-3p	7.78	7.23	down	1.69×10^{-04}	**up** (Cogswell et al., 2008)**; down** (Wang et al., 2011)
hsa-miR-10b	10.45	9.21	down	6.39×10^{-04}	down (Lau et al., 2013)
hsa-miR-592	6.10	5.30	down	6.81×10^{-04}	
hsa-miR-129-3p	12.95	12.30	down	1.21×10^{-03}	down (Lau et al., 2013; Wang et al., 2011)
hsa-miR-590-5p	6.47	5.97	down	1.63×10^{-03}	
hsa-miR-22	9.73	9.29	down	2.23×10^{-03}	down (Hébert et al., 2008; Wang et al., 2011)
hsa-miR-1274b	8.59	9.70	up	3.00×10^{-03}	
hsa-miR-323-3p	9.49	9.13	down	3.45×10^{-03}	
hsa-miR-543	6.28	5.59	down	3.47×10^{-03}	down (Lau et al., 2013)
hsa-miR-664	10.96	12.06	up	3.77×10^{-03}	
hsa-miR-143	10.76	11.57	up	3.86×10^{-03}	**down** (Wang et al., 2011)**; up** (Cogswell et al., 2008)
hsa-miR-195	12.79	13.29	up	4.43×10^{-03}	**down** (Wang et al., 2011)**; up** (Lau et al., 2013)
hsa-miR-369-5p	5.78	4.69	down	4.72×10^{-03}	
hsa-miR-3122	6.11	4.94	down	4.86×10^{-03}	
hsa-miR-148b	8.61	8.28	down	5.90×10^{-03}	**down** (Nunez-Iglesias et al., 2010; Wang et al., 2011)**; up** (Cogswell et al., 2008)
hsa-miR-1289	6.22	5.51	down	6.25×10^{-03}	
hsa-miR-876-5p	10.38	11.26	up	6.43×10^{-03}	
hsa-miR-129-5p	7.16	5.97	down	6.51×10^{-03}	down (Lau et al., 2013; Wang et al., 2011)
hsa-miR-4270	9.44	10.25	up	7.23×10^{-03}	
hsa-miR-409-5p	9.24	8.82	down	8.61×10^{-03}	down (Lau et al., 2013)
hsa-miR-584	5.81	4.69	down	8.77×10^{-03}	down (Wang et al., 2011)
hsa-miR-449c*	8.65	8.38	down	9.39×10^{-03}	
hsa-miR-296-3p	6.93	7.95	up	9.42×10^{-03}	
hsa-miR-1972	8.74	9.34	up	1.14×10^{-02}	
hsa-miR-126	11.47	11.04	down	1.14×10^{-02}	down (Wang et al., 2011)
hsa-miR-490-5p	6.60	6.17	down	1.14×10^{-02}	
hsa-miR-148b*	10.00	9.79	down	1.16×10^{-02}	
hsa-miR-3943	7.61	7.04	down	1.22×10^{-02}	
hsa-miR-554	5.75	4.76	down	1.27×10^{-02}	
hsa-miR-3922	9.38	9.06	down	1.36×10^{-02}	
hsa-miR-1324	5.74	6.66	up	1.36×10^{-02}	
hsa-miR-186*	6.09	5.46	down	1.37×10^{-02}	
hsa-miR-191	9.54	9.13	down	1.40×10^{-02}	down (Cogswell et al., 2008; Wang et al., 2011)
hsa-miR-138	11.26	11.01	down	1.41×10^{-02}	down (Lau et al., 2013; Wang et al., 2011)
hsa-miR-3665	6.14	5.70	down	1.50×10^{-02}	
hsa-miR-7	6.80	5.53	down	1.53×10^{-02}	**down** (Wang et al., 2011)**; up** (Cogswell et al., 2008)
hsa-miR-3074	9.49	8.87	down	1.55×10^{-02}	
hsa-let-7i	6.52	5.98	down	1.58×10^{-02}	**down** (Hébert et al., 2008; Wang et al., 2011)**; up** (Lau et al., 2013)
hsa-miR-200a	6.14	5.58	down	1.61×10^{-02}	**up** (Lau et al., 2013)
hsa-miR-32	5.79	5.13	down	1.61×10^{-02}	down (Wang et al., 2011)
hsa-miR-152	8.70	8.78	up	1.61×10^{-02}	
hsa-miR-484	9.09	8.54	down	1.64×10^{-02}	
hsa-miR-3202	6.01	6.59	up	1.65×10^{-02}	
hsa-miR-596	6.87	6.67	down	1.73×10^{-02}	
hsa-miR-1246	4.67	5.84	up	1.89×10^{-02}	

hsa-miR-500a	5.81	6.94	up	$1.91x10^{-02}$	
hsa-miR-1200	6.46	6.16	down	$1.91x10^{-02}$	
hsa-miR-92a-2*	4.67	5.65	up	$2.00x10^{-02}$	
hsa-miR-762	9.83	10.57	up	$2.02x10^{-02}$	
hsa-miR-3621	8.03	8.56	up	$2.05x10^{-02}$	
hsa-miR-324-5p	8.81	8.39	down	$2.08x10^{-02}$	**up** (Cogswell et al., 2008)
hsa-miR-519d	8.53	9.13	up	$2.16x10^{-02}$	**down** (Wang et al., 2011)**; up** (Cogswell et al., 2008)
hsa-miR-486-5p	7.49	6.99	down	$2.19x10^{-02}$	**up** (Nunez-Iglesias et al., 2010)
hsa-miR-3622b-3p	7.40	7.14	down	$2.22x10^{-02}$	
hsa-miR-1234	8.51	8.15	down	$2.24x10^{-02}$	
hsa-miR-517b	5.23	6.09	up	$2.29x10^{-02}$	
hsa-miR-4307	5.79	4.69	down	$2.33x10^{-02}$	
hsa-miR-3605-5p	5.87	6.40	up	$2.34x10^{-02}$	
hsa-miR-29b-2*	5.85	5.01	down	$2.38x10^{-02}$	
hsa-miR-3141	11.02	11.98	up	$2.41x10^{-02}$	
hsa-miR-3941	9.09	9.70	up	$2.43x10^{-02}$	
hsa-miR-628-3p	7.85	7.36	down	$2.47x10^{-02}$	
hsa-miR-3199	5.65	5.15	down	$2.48x10^{-02}$	
hsa-miR-376c	9.14	8.67	down	$2.49x10^{-02}$	down (Nunez-Iglesias et al., 2010; Wang et al., 2011)
hsa-miR-183*	9.37	9.73	up	$2.53x10^{-02}$	
hsa-miR-523	8.12	7.40	down	$2.64x10^{-02}$	
hsa-miR-196b*	5.75	6.39	up	$2.72x10^{-02}$	
hsa-miR-30c	5.92	6.33	up	$2.72x10^{-02}$	**down** (Cogswell et al., 2008; Wang et al., 2011)**; up** (Cogswell et al., 2008)
hsa-miR-3909	8.55	8.96	up	$2.83x10^{-02}$	
hsa-miR-144	6.27	5.94	down	$2.87x10^{-02}$	**up** (Wang et al., 2011)
hsa-miR-610	8.54	8.07	down	$2.91x10^{-02}$	
hsa-miR-497*	6.12	5.94	down	$2.93x10^{-02}$	
hsa-miR-943	6.75	7.06	up	$2.93x10^{-02}$	
hsa-miR-548t	6.02	6.76	up	$2.94x10^{-02}$	
hsa-miR-4295	7.85	7.44	down	$3.06x10^{-02}$	
hsa-miR-3622b-5p	7.46	7.98	up	$3.07x10^{-02}$	
hsa-miR-550a	5.63	5.92	up	$3.08x10^{-02}$	
hsa-miR-3124	7.84	7.12	down	$3.11x10^{-02}$	
hsa-miR-518c	8.44	8.10	down	$3.11x10^{-02}$	
hsa-miR-1228*	10.25	11.08	up	$3.14x10^{-02}$	
hsa-miR-2117	5.42	5.99	up	$3.30x10^{-02}$	
hsa-miR-423-5p	7.99	8.65	up	$3.33x10^{-02}$	**down** (Wang et al., 2011)
hsa-miR-200b*	8.54	8.31	down	$3.34x10^{-02}$	
hsa-miR-4276	6.46	6.16	down	$3.34x10^{-02}$	
hsa-miR-9*	12.06	11.74	down	$3.36x10^{-02}$	
hsa-miR-302c	5.39	6.34	up	$3.43x10^{-02}$	
hsa-miR-675	7.34	7.74	up	$3.48x10^{-02}$	
hsa-miR-515-5p	6.46	6.12	down	$3.51x10^{-02}$	
hsa-miR-301b	6.48	6.80	up	$3.64x10^{-02}$	
hsa-miR-191*	5.66	4.15	down	$3.93x10^{-02}$	
hsa-miR-514b-3p	7.57	7.81	up	$4.03x10^{-02}$	
hsa-miR-635	6.71	6.33	down	$4.24x10^{-02}$	
hsa-miR-603	6.86	6.34	down	$4.26x10^{-02}$	
hsa-miR-1293	5.08	5.89	up	$4.36x10^{-02}$	
hsa-miR-608	7.41	8.17	up	$4.46x10^{-02}$	
hsa-miR-149*	9.84	10.45	up	$4.61x10^{-02}$	
hsa-miR-3689a-5p	10.25	9.66	down	$4.63x10^{-02}$	
hsa-miR-3911	5.42	5.94	up	$4.70x10^{-02}$	
hsa-miR-3133	7.51	7.84	up	$4.78x10^{-02}$	
hsa-miR-875-3p	8.20	7.94	down	$4.99x10^{-02}$	

Table 3: Genome wide significantly deregulated mRNAs and their correlation to hsa-miR-132-3p and hsa-miR-212-3p expression levels in TC samples of AD patients

Expression levels of genome wide significantly deregulated mRNAs (9 up- and 1 downregulated in AD). Expression levels were correlated with expression levels of genome wide significant miRNAs by linear regression. Given p-values are unadjusted. p-values marked with (‡) passed Bonferroni correction for 11 264 analyzed markers (p-value < 4.4×10^{-06}).

Gene Symbol	student's T-test diagnosis~mRNA p-value	trend in AD	miR-132/212 target prediction sites	linear regression mRNA~hsa-miR-132-3p		linear regression mRNA~hsa-miR-212-3p	
				p-value	R^2	p-value	R^2
RNU1G2	1.51×10^{-09}	up	none	6.49×10^{-05}	0.276	$1.54 \times 10^{-07(‡)}$	0.447
RNU1-3	4.37×10^{-09}	up	none	9.88×10^{-05}	0.264	$7.27 \times 10^{-08(‡)}$	0.464
RNU1-5	1.55×10^{-08}	up	none	1.12×10^{-04}	0.260	$1.15 \times 10^{-07(‡)}$	0.453
AEBP1	9.74×10^{-08}	up	none	$1.79 \times 10^{-07(‡)}$	0.423	$7.56 \times 10^{-08(‡)}$	0.463
NFKB1	1.44×10^{-07}	up	**hsa-miR-132-3p**	$1.03 \times 10^{-07(‡)}$	0.435	1.17×10^{-05}	0.338
PKN2	6.34×10^{-07}	up	**hsa-miR-132-3p hsa-miR-212-3p**	1.78×10^{-04}	0.247	7.11×10^{-06}	0.352
HBP1	7.51×10^{-07}	up	none	$8.84 \times 10^{-08(‡)}$	0.439	4.80×10^{-05}	0.300
C5ORF41	8.90×10^{-07}	up	**hsa-miR-132-3p hsa-miR-212-3p**	4.39×10^{-04}	0.221	2.02×10^{-03}	0.185
TSPAN7	3.32×10^{-06}	down	none	$8.76 \times 10^{-08(‡)}$	0.439	$3.93 \times 10^{-07(‡)}$	0.425
GFAP	3.70×10^{-06}	up	**hsa-miR-132-3p hsa-miR-212-3p**	$5.14 \times 10^{-09(‡)}$	0.458	$1.93 \times 10^{-08(‡)}$	0.493

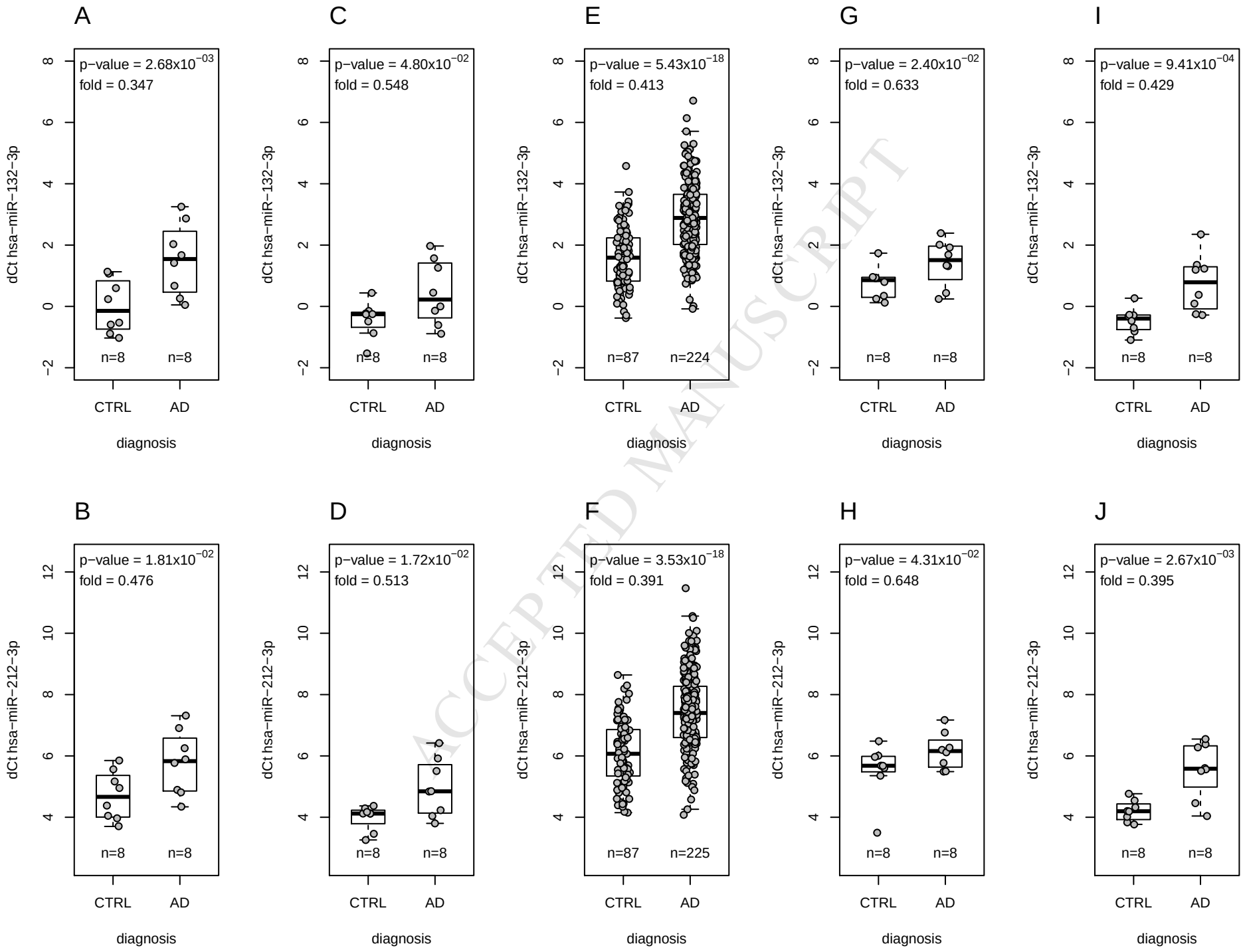

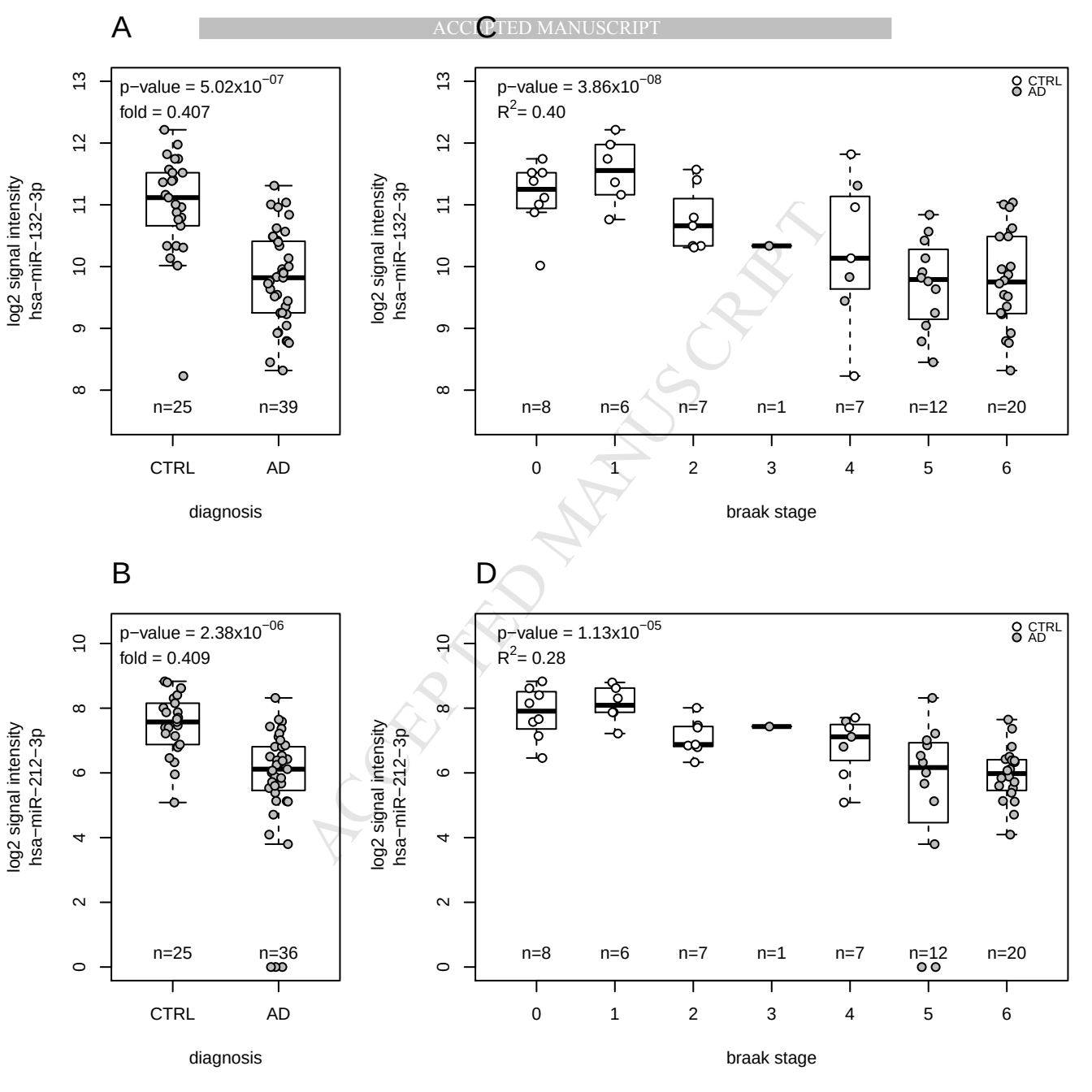

HIGHLIGHTS

- Simultaneous microRNA and RNA analysis in a large AD/control sample set
- miR-132/212 decrease in cortical brain regions correlated with disease progression
- stronger miR-132/212 decrease in grey compared to white matter tissue of AD patients
- genome wide significance for small nuclear RNAs recently associated to AD
- correlation of significantly deregulated miRNAs and mRNAs (*in silico)*